

# **SIMULATION OF BEHAVIOR OF REINFORCED CONCRETE COLUMNS SUBJECTED TO CYCLIC LATERAL LOADS**

**H. Sezen<sup>1</sup>, M.S. Lodhi<sup>2</sup>, E. Setzler<sup>3</sup>, and T. Chowdhury<sup>4</sup>**

*<sup>1,2</sup>Department of Civil and Environmental Engineering and Geodetic Science,  
The Ohio State University, Columbus, Ohio*

*<sup>3</sup>Burgess and Niple, Painesville, Ohio*

*<sup>4</sup>Skidmore Owings and Merrill, Chicago, Illinois*

## **ABSTRACT**

Reinforced concrete (RC) columns with insufficient transverse reinforcement and non-seismic reinforcement details are vulnerable to shear failure and loss of axial load carrying capacity. With an aim of developing a macro model to simulate cyclic lateral load-deformation performance, the behavior of non-ductile RC columns is modeled by combining deformation components due to flexure, reinforcement slip and shear. Individual deformation component models developed for monotonic lateral loads serve as envelopes or primary curves for respective cyclic responses. Based on a comparison of their predicted shear and flexural strengths, the columns are classified into five general categories and total monotonic and cyclic response is obtained by combining the three deformation components according to a set of rules specified for each category. The proposed monotonic and cyclic response models are compared with the data from various experimental studies on columns having flexural failure with very limited or no shear effects, flexure and/or shear failure following the flexural yielding, and shear failure prior to flexural yielding. The predicted and experimental response of columns failing primarily in shear and flexure were comparable. Similarly, the hysteretic response of the column with axial load failure was captured reasonably well by forcing the monotonic response envelopes to degrade linearly between the peak strength and the point of axial load failure. Although, the research is focused on modeling the behavior of shear critical columns under seismic loads, the developed model is applicable to all RC columns.

**KEYWORDS:** Reinforced concrete columns, monotonic and cyclic load, shear failure, axial load failure, load-deformation behavior.

## **1. INTRODUCTION**

There is a large inventory of reinforced concrete buildings in US and other parts of the world that are not designed according to modern seismic design provisions. These buildings are often characterized by low lateral displacement capacity and rapid degradation of shear strength and hence are vulnerable to severe damage or even collapse during strong ground motions. The need to assess their vulnerability to earthquake damage and hence suggesting the desired level of retrofit requires evaluation of the expected behavior in terms of strength and deformation capacity. Reconnaissance of damage observed during the past earthquakes suggests that poorly designed reinforced concrete columns are the most critical elements to sustain damage leading to a potential building collapse (Sezen et al. 2003). Typically, these columns have insufficient and widely spaced transverse reinforcement and lack essential seismic reinforcement details resulting in non ductile behavior. The research reported here is aimed at developing a model that can predict monotonic and cyclic response of a lightly reinforced concrete column subjected to lateral loading.

A typical fixed-ended reinforced concrete column, when subjected to earthquake loading, undergoes lateral deformation which is comprised of three components; flexural deformations, reinforcement slip deformations and

shear deformations (Fig 1a). Each of these deformation components are modeled separately and then combined under a set of rules to obtain total monotonic and cyclic lateral response. Component deformation models and total response model under monotonically increasing lateral load serve as response envelope or primary curve for respective component and cyclic responses. The proposed model is tested against the experimental data reported by various researchers and is found to perform well with sufficient accuracy. Although, the research is focused on modeling lightly reinforced concrete columns that experience flexural yielding followed by the shear failure, the model is applicable to the columns failing in shear such as very short columns or well reinforced columns that develop plastic hinges and eventually fail in flexure.

## 2. DEVELOPMENT OF MONOTONIC LATERAL RESPONSE ENVELOPE

### 2.1. Flexural Deformations

Flexural response of reinforced concrete elements can accurately be determined by performing section analysis on a fiber model considering the actual constitutive material properties in one dimensional stress field. In this study, the constitutive laws for concrete in compression are defined considering the effects of confinement on concrete core as per the confinement model by Mander et al. (1988). However, in order to represent the expected post-peak concrete behavior in shear critical columns, the descending branch is modeled by the relation developed by Roy and Sozen (1964). The reinforcing steel behavior is modeled considering a linear elastic behavior, a yield plateau, and a non-linear strain-hardening region. To be as realistic as possible and to capture non-linearity in actual curvature distribution, flexural deformations are calculated by integrating curvatures up to the yield point and by a plastic hinge model after the yielding as per Eqn 2.1.1 and 2.1.2 respectively.

$$\Delta_{f,y} = \int_0^L \phi(x) x dx \quad (2.1.1)$$

$$\Delta_f = \Delta_{f,y} + (\phi - \phi_y) L_p \left( a - \frac{L_p}{2} \right) \quad (2.1.2)$$

where  $\Delta_{f,y}$  is the flexural displacement at yield,  $\phi(x)$  is the section curvature at distance  $x$  measured along column axis,  $L$  is the height of the column,  $\phi$  is the curvature at the column end,  $\phi_y$  is the curvature at yield, and  $a$  is the shear span. The plastic hinge length,  $L_p$ , is taken as one half of the total section depth per the recommendations of Moehle (1992). Complete details of the flexural deformation model, including the material constitutive laws and moment-curvature analysis, can be found in Setzler (2005) and Chowdhury (2007).

### 2.2. Reinforcement Slip Deformation

The flexural deformations as determined through conventional fiber section analysis do not account for the rotations that are caused by reinforcement slip. This results in lateral displacement that can be as large as 25 to 40% of the total lateral deformations (Sezen, 2002). Therefore, slip deformations must be accounted for separately and added to the other deformation components (flexure and shear) to accurately model total drift of a column. Lateral displacements due to reinforcement slip are calculated in this study through a model which was originally developed by Sezen and Moehle (2003) and further developed by Sezen and Setzler (2008). The model, as shown in Fig 2a, approximates the bond stress as bi-uniform function with different values for elastic and inelastic steel behavior, which allows for the efficient computation of the reinforcement slip and eliminates the need for the nested

iteration loops that are required in some of the existing bond stress-slip models. The value for the bond stress in the elastic range is taken as  $u_b = 1\sqrt{f'_c}$  (MPa) based on a study by Sezen (2002) on 12 test columns. For the inelastic range, the value for bond stress is adopted from the study by Lehman and Moehle (2000) as  $u'_b = 0.5\sqrt{f'_c}$  (MPa) where  $f'_c$  is concrete compressive strength. Slip at the loaded end of the reinforcing bar can be calculated by integrating bi-linear strain distribution over the development length as follows:

$$slip = \int_0^{l_d+l'_d} \varepsilon(x)dx \quad (2.2.1)$$

where  $l_d = \frac{f_s d_b}{4u_b}$  and  $l'_d = \frac{(f_s - f_y) d_b}{4u'_b}$  correspond to the development lengths for elastic and inelastic portions of the bar, respectively.  $f_s$  is stress at loaded end of the bar,  $f_y$  and  $d_b$  are yield stress and diameter of the bar, respectively. The reinforcement slip is assumed to occur in tension bars only and cause the rotation about the neutral axis. Hence, slip rotation can be calculated from the following equation:

$$\theta_s = \frac{slip}{d - c} \quad (2.2.2)$$

where  $d$  and  $c$  are the distances from the extreme compression fiber to the centroid of the tension steel and the neutral axis, respectively. The lateral displacement at the free end of a cantilever column can be calculated as the product of this slip rotation and length of the column.

### 2.3. Shear Deformations

The basis of the shear model used in this research is the model developed by Patwardhan (2005), which uses Modified Compression Field Theory, MCFT (Vecchio and Collins, 1986). Patwardhan (2005) proposed a piecewise linear model defining key points in the lateral force-shear deformation envelope through a parametric study implementing MCFT through a computer program Response-2000. In this study, pre-peak non linear shear force-shear deformation response is obtained indirectly from Response-2000 by integrating shear strain distribution over the height of the column for each load step as following:

$$\Delta_v = \int_0^L \gamma(x)dx \quad (2.3.1)$$

where  $\gamma$  is the average shear strain over the cross-section at each location  $x$  along the height,  $L$  of the column, and  $\Delta_v$  is the shear displacement. After the peak strength has reached, the shear strength is assumed to remain constant at its peak value until the onset of shear strength degradation. By modifying the equation proposed by Gerin and Adebar (2004), the shear displacement at the onset of shear degradation,  $\Delta_{v,u}$ , can be calculated as:

$$\Delta_{v,u} = \left( 4 - 12 \frac{v_n}{f'_c} \right) \Delta_{v,n} \quad (2.3.2)$$

Where,  $v_n$  is the shear stress at peak strength,  $f'_c$  is the concrete compressive strength, and  $\Delta_{v,n}$  is the shear displacement at maximum strength determined from Response-2000. The peak strength,  $V_{peak}$  is the minimum of the shear strength of the column,  $V_n$ , and shear force corresponding to the maximum moment sustainable by the section,  $V_p$ . After the shear degradation is initiated, shear strength decreases linearly with increasing shear deformations to the point of axial load failure, where lateral strength is assumed to be zero, as shown in Fig 2b. The displacement at axial load failure,  $\Delta_{v,f}$ , is calculated as:

$$\Delta_{v,f} = \Delta_{ALF} - \Delta_{f,f} - \Delta_{s,f} \geq \Delta_{v,u} \quad (2.3.3)$$

where  $\Delta_{ALF}$  is the total displacement at axial load failure, and  $\Delta_{f,f}$  and  $\Delta_{s,f}$  are the flexural and slip displacements, respectively, at the point of axial load failure. The drift at axial load failure is determined by the expression proposed by Elwood and Moehle (2005a), which is based on a shear friction model and an idealized shear failure plane as:

$$\frac{\Delta_{ALF}}{L} = \frac{4}{100} \frac{1 + \tan^2 \theta}{\tan \theta + P \left( \frac{s}{A_{sv} f_{yv} d_c \tan \theta} \right)} \quad (2.3.4)$$

where  $\theta$  is the angle of the shear crack,  $P$  is the axial load,  $A_{sv}$  is the area of transverse steel with yield strength  $f_{yv}$  at spacing  $s$ , and  $d_c$  is the depth of the core concrete, measured to the centerlines of the transverse reinforcement. In the derivation,  $\theta$  is assumed to be 65 degrees.

#### 2.4. Total Monotonic Lateral Response

The proposed procedure models each of flexure, slip and shear deformation by a spring subjected to the same force and the total response is the sum of the responses of each spring (Fig 1b). Each of the deformation components can simply be added to obtain the total response up to the peak strength of the column. However, for post-peak behavior, the column is classified into one of the five categories based on a comparison of its shear, yield and flexural strengths and rules are specified for the combination of the deformation components for each category (Setzler and Sezen, 2008). Yield strength,  $V_y$  is defined as the lateral load corresponding to the first yielding of the tension bars in the column, flexural strength,  $V_p$  is the lateral load corresponding to the peak moment sustainable by the column during flexural analysis. The shear strength of the column,  $V_n$  is calculated by the expression developed by Sezen and Moehle (2004) for lightly reinforced concrete columns as:

$$V_n = k(V_c + V_s) = k \left[ \left( \frac{6\sqrt{f'_c}}{a/d} \sqrt{1 + \frac{P}{6\sqrt{f'_c} A_g}} \right) 0.80 A_g + \frac{A_{sv} f_{yv} d}{s} \right] \quad (2.4.1)$$

where  $V_c$  is the concrete contribution to shear strength,  $V_s$  is the steel contribution to shear strength.  $A_{sv}$  is the area of transverse steel at spacing  $s$ ,  $k$  is a factor related to the displacement ductility  $\mu$ , which is the ratio of the maximum displacement to the yield displacement.

Classification of the column based on comparison of shear, yield and flexural strength determines expected column behavior. The peak response is limited by the lesser of the shear strength ( $V_n$ ) and the flexural strength ( $V_p$ ), however post peak response is assumed to be governed by the limiting mechanism (i.e., flexure or shear). Category

I column ( $V_n < V_y$ ) fails in shear while the flexural behavior remains elastic. Category II column ( $V_y \leq V_n < 0.95V_p$ ) also fails in shear, however inelastic flexural deformation occurring prior to shear failure affects the post-peak behavior. Shear deformations continue to increase after the peak shear strength is reached, but the flexure and shear springs are locked at their peak strength values. In Category III column ( $0.95V_p \leq V_n \leq 1.05V_p$ ), the shear and flexural strengths are nearly identical. It is not possible to predict conclusively which mechanism will govern the peak response. Shear and flexural failure are assumed to occur “simultaneously,” and both mechanisms contribute to the post-peak behavior. Category IV column ( $1.05V_p < V_n \leq 1.4V_p$ ) may potentially fail in the flexure, however inelastic shear deformations affect the post-peak behavior and shear failure may occur as the displacements increase. The shear strength in Category V column ( $V_n > 1.4V_p$ ) is much greater than the flexural strength and column fails in flexure while shear behavior remains elastic.

### 2.5. Shear Failure at High Displacement Ductility

Shear strength degrades as the displacement ductility increases (Sezen and Moehle, 2004), which can cause shear failure in the columns that are initially dominated by flexure. To capture such behavior, as encountered in category-IV columns, shear failure surface defined by the empirical drift capacity model by Elwood and Moehle (2005b) is imposed on the lateral load-total displacement behavior as per following equation:

$$\frac{\Delta_{SF}}{L} = \frac{3}{100} + 4\rho_v - \frac{1}{500} \frac{v}{\sqrt{f'_c}} - \frac{1}{40} \frac{P}{A_g f'_c} \geq \frac{1}{100} \quad (2.5.1)$$

where  $\Delta_{SF}$  is the drift at shear failure,  $\rho_v$  is the transverse reinforcement ratio, and  $v$  is the nominal shear stress.  $f'_c$  and  $v$  have units of psi. If the total lateral response envelope exceeds the calculated drift at shear failure, shear failure is assumed to have occurred (Elwood 2004), and the model is modified to degrade linearly from the point of shear failure to strength of zero at the drift at axial load failure.

## 3. CYCLIC RESPONSE MODEL

Lightly reinforced concrete columns exhibit characteristic behavior under cyclic lateral loading associated with stiffness deterioration, strength decay, pinching, and axial load effects. A realistic hysteretic model must be able to simulate these characteristic features in order to successfully predict the lateral deformation response of such columns. As was done for monotonic response, cyclic response for each deformation component is predicted using a set of hysteretic rules and then combined to obtain total cyclic response. Each component and total monotonic response serves as an envelope or primary curve for the corresponding cyclic response component. The proposed cyclic response models are based on existing hysteretic models that are either simplified for computational efficiency or modified to better present the actual behavior of the columns considered in this study.

### 3.1. Component Hysteretic Models

In order to accurately analyze the hysteretic flexural response a shear critical column, strength decay features must be incorporated into hysteretic model alongwith stiffness degradation considerations. The proposed hysteretic model for flexural response is based on a modified model by Takeda et al. (1970), which provides realistic lateral behavior of reinforced concrete column with a limited computational effort and incorporates degradation of stiffness during reloading and unloading of hysteretic force-deformation behavior. In the proposed model, the reloading branches of hysteretic loops are aimed at previous maximum response points, thereby simulating stiffness degradation. The reloading slope ( $k_3$  in Fig 4a) is decreased with increasing maximum response deformation.

Unloading slopes ( $k_1$  and  $k_2$  in Fig 4a) are calculated as a function of the previous maximum deformation. The original unloading slope defined by Takeda et al. (1970) is multiplied by a factor of 1.7 to predict realistic cyclic flexural response of a lightly reinforced concrete column. Hence, the proposed slope of the unloading branch is given by:

$$k_r = 1.7k_y \left( \frac{D_y}{D} \right)^{0.4} \quad (3.1.1)$$

where  $k_r$  is the slope of the unloading branch,  $k_y$  is the slope of the line connecting the yield point in one direction to the cracking point in the other direction,  $D$  is the maximum deflection attained in the direction of the loading, and  $D_y$  is the yield deflection. The strength decay feature is incorporated in the proposed cyclic flexural model by enveloping the response through monotonic flexural response which exhibits deterioration of strength after reaching the peak strength. For simplicity, the calculated monotonic response envelope is represented by few selected points on the envelope and extended linearly beyond the theoretical failure point. This envelope replaces tri-linear primary curve used in original Takeda et al. model.

The proposed hysteretic model for reinforcement slip is based on the model by Alsiwat and Saatcioglu (1992) which incorporates pinching of hysteresis loops and degradation of stiffness taking place during reloading and unloading. The primary curve employed for the hysteretic model by Alsiwat and Saatcioglu is replaced with monotonic response envelope based on the bar slip model proposed by Sezen and Setzler (2008). The slopes of the unloading and reloading branches change only at zero force level, hence proposed hysteretic slip model is similar to that of hysteretic flexural model shown in Fig 4a. The monotonic slip model envelopes the hysteretic model and forces strength decay beyond peak strength at larger deformations.

Unlike flexural response, shear force-shear deformation relationship shows pronounced pinching of hysteresis loops due to sliding of two cracked surfaces, developed during previous loadings, and is exhibited by a reduction in load resistance during reloading. Shear critical reinforced concrete columns also exhibit prominent deterioration in stiffness and strength decay during reversed cyclic loading. The proposed hysteretic shear model is based on the model by Ozcebe and Saatcioglu (1989) which successfully integrates strength decay, stiffness deterioration and pinching of hysteresis loops in hysteretic shear force-shear deformation relationship in a computationally efficient way. The pinching of hysteresis loops is incorporated in the model by defining two separate lines for reloading branches, with a change of slope established at the cracking point or  $V_{cr}$  in Fig 4b. The deterioration of the stiffness is simulated by aiming at previous maximum response points. The model by Ozcebe and Saatcioglu is modified to better simulate stiffness degradation and to capture response of the column with limited displacement ductility or with no flexural yielding. In this regard, it is suggested that the reloading branch be targeted at the previous peak displacement and load instead of a projected point in the original model. Thus the reloading branch beyond  $V_{cr}$  follows a straight line and passes through the maximum displacement point reached previously. Also, in order to capture response of the column with significant shear distress properly, the slope of the unloading branch between  $V_{cr}$  and zero lateral load ( $k_2$  or  $k'_2$  in Fig 4b) is revised and reduced to:

$$k_2 \text{ or } k'_2 = 0.2k_y \left( 1 - 0.07 \frac{\Delta}{\Delta_y} \right) \quad (3.3.1)$$

where  $\Delta$  is maximum displacement reached during previous cycle before unloading,  $\Delta_y$  is deflection at yield, and  $k_y$  is slope at yielding.

### **3.2. Combined Hysteretic Model/Total Cyclic Response**

The total cyclic response of reinforced concrete column is predicted by coupling the hysteretic flexure, reinforcement slip, and shear responses as springs in series. The force in each spring is always same and total displacement is sum of the displacements of each spring. Up to the peak strength of the column and during unloading and reloading branches, three deformation components are simply added to calculate total lateral displacement. After the peak response is obtained, either shear or flexure governs the column behavior. Post-peak total hysteretic response is bounded by the total monotonic response based on column failure mode or classification category.

## **4. COMPARISON OF MODELS AND TEST DATA**

### **4.1. Monotonic Response Model**

In order to verify the proposed model and test its applicability to a wider range of shear and flexural strengths, material properties and column geometries, a database of 37 column tests from eight different researchers was compiled from Pacific Earthquake Engineering Research Center's Structural Performance Database. Lateral force-displacement relationships are shown in Fig 3 for five of the 37 test columns (one from each category) modeled in this study. Comparisons for the other columns can be found in Setzler (2005). The plots compare the response envelopes predicted by the proposed model to cyclic test data for each column. The model predicts reasonable response envelopes for the columns examined in the study. For columns in Category IV (Fig 3d) the dashed lines show the proposed model before modification for delayed shear failure. The solid line is the final model prediction, after consideration of the Elwood shear failure surface. The shear failure surface was used successfully in predicting the lateral response of Category IV columns. As discussed previously, Category V columns are those whose shear strengths are high enough such that they are not expected to experience shear failure even at large displacements. The Elwood shear failure surface and point of axial failure were computed for these columns for comparison purposes. However, for category V columns, it is not appropriate to modify the model using the Elwood shear failure surface as the proposed model predicts the behavior of these columns well without any shear failure modifications.

### **4.2. Cyclic Response Model**

Fig 5 shows the comparison of experimental and predicted response of columns tested by Sezen and Moehle (2006). Specimen-1 is a Category III column. It should be noted that the range of experimental and predicted displacement response is between -90 and +80 mm, however this column was able to carry its axial load at larger lateral displacements. The cyclic model had to be stopped at a lower displacement mainly because the experimental flexure, bar slip, and shear displacements were not available beyond what is measured. The total experimental lateral displacement is measured by a single displacement potentiometer or LVDT attached to the top of the column specimen. However, the component experimental hysteretic displacements were obtained from up to 62 different displacement potentiometers. Thus, the sum of individual experimental displacements do not necessarily equal to the total experimental displacement. As a result of this discrepancy in the experimental data, the maximum predicted and experimental lateral displacements are sometimes not close. If the sum of measured component displacements matched the total lateral displacement, the predicted hysteretic response would improve greatly. To the authors' knowledge, there is very limited or no experimental column studies reporting individual hysteretic flexure, bar slip and shear displacements. Specimen-2 is classified as a Category IV column, failing in flexure with limited contributions from shear at failure. Specimen-3 was tested under variable axial load. In the positive loading

direction it is a Category IV column, while in the negative direction it is placed in Category III. Specimen-4 is identical to Specimen-1, and belongs to Category III. It is evident that reasonable correlation exists between analytical and experimental results. The proposed hysteretic model captures the strength decay in columns. Although the strength of the columns predicted reasonably, the overall response was not predicted well in many cycles mainly because the sum of experimental component displacements used in the model did not match the total experimental lateral displacement. Complete details of comparisons alongwith application of proposed hysteretic model to other specimen can be found in Chowdhury (2007).

## 5. CONCLUSIONS

An analytical macro model is developed that can simulate non linear monotonic and cyclic response of reinforced concrete columns. Although, the research was focused on studying the behavior of shear critical columns, the proposed models can accurately predict the lateral force-displacement response of well designed columns as well. Deformation components due to flexure, reinforcement slip and shear are first modeled individually for monotonic loading and then combined depending upon comparison of their shear and flexural strength. The component and total monotonic response models envelop the corresponding cyclic behavior in the development of cyclic response models. The proposed monotonic and cyclic response models are tested against a database of test specimens. The comparison of monotonic response model with the test data shows reasonable agreement in predicting the maximum strength of the columns and their failure mode. The average of the ratio of predicted strength to experimental strength was 0.95 with a standard deviation of 0.10. Similarly, for cyclic response models, strength decay behavior was reasonably captured by forcing the response to follow the deterioration of strength in monotonic envelope after peak strength is achieved. The classification system used appears to identify the failure mode and represent the flexural and shear behavior for cyclic response as well.

## REFERENCES

- Alsawat, J.M., Saatcioglu, M. Reinforcement Anchorage Slip under Monotonic Loading. *ASCE Journal of Structural Engineering*. 1992; **118** (9) 2421-2438.
- Chowdhury, T. Hysteretic Modeling of Shear-Critical Reinforced Concrete Columns. *M.S. Thesis*. The Ohio State University, Columbus, Ohio, 2007.
- Elwood, J.K., Moehle, J.P. Shake Table Tests and Analytical Studies on the Gravity Load Collapse of Reinforced Concrete Frames. *PEER Report 2003/01*, Pacific Earthquake Engineering Research Center, Univ. of California, Berkeley, 2003.
- Elwood, K. J., Moehle, J.P. Drift Capacity of Reinforced Concrete Columns with Light Transverse Reinforcement. *Earthquake Spectra*. 2005; **21** (1), 71-89.
- Elwood, K.J., Moehle J.P. Axial Capacity Model for Shear-Damaged Columns. *ACI Structural Journal*. 2005; **102** (4), 578-587
- Gerin, M., Adebar, P. Accounting for Shear in Seismic Analysis of Concrete Structures. *Proceedings of the 13<sup>th</sup> World Conference on Earthquake Engineering*, Vancouver, 2004. Paper No. 1747  
<http://www.ecf.utoronto.ca/~bentz/home.shtml> (last visited on Nov. 15, 2007)



- Lee, D.H., Elnashai, A.S. Seismic Analysis of RC Bridge Columns with Flexure- Shear Interaction. *ASCE Journal of Structural Engineering* 2001; **127** (5): 546-553.
- Lehman, D.E., Moehle, J.P. Seismic Performance of Well-Confined Concrete Bridge Columns. *PEER Report 98/01*, Pacific Earthquake Engineering Research Center, Univ. of California, Berkeley, 2000. 316 pp.
- Lynn, A.C., Moehle, J.P., Mahin, S.A., Holmes, W.T. Seismic Evaluation of Existing Reinforced Concrete Building Columns. *Earthquake Spectra* 1996; **124** (4) 715–739.
- Mander, J.B., Priestley, J.N., Park, R. Theoretical Stress-Strain Model for Confined Concrete. *ASCE Journal of Structural Engineering*. 1988; **114** (8), 1804-1825.
- Ozcebe, G., Saatcioglu, M. Hysteretic Shear Model for Reinforced Concrete Members. *ASCE Journal of Structural Engineering*. 1989; **115** (1), 132-148.
- Patwardhan, C. Strength and Deformation Modeling of Reinforced Concrete Columns. *M.S. Thesis*. The Ohio State University, Columbus, Ohio, 2005.
- Petrangeli, M., Pinto P.E., Ciampi V. Fiber Element for Cyclic Bending and Shear of RC Structures. I: Theory. *ASCE Journal of Engineering Mechanics* 1999; **125** (9): 994-1001
- Pincheira, J.A., Dotiwala, F.S., D’Souza, J.T. Seismic Analysis of Older Reinforced Concrete Columns. *Earthquake Spectra* 1999; **15** (2): 245-272.
- Ricles, J.M., Yang, Y.S., Priestley, M.J.N. Modeling Nonductile R/C Columns for Seismic Analysis of Bridges. *ASCE Journal of Structural Engineering* 1998; **124** (4): 415-425.
- Roy, H.E.H., Sozen, M.A. Ductility of Concrete. *International Symposium on Flexural Mechanics of Reinforced Concrete - Proceedings*. Miami, Fla., 1964. 213-235.
- Saatcioglu, M., Ozcebe, G. Response of Reinforced Concrete Columns to Simulated Seismic Loading. *ACI Structural Journal* 1989; **86** (1) 3-12.
- Saatcioglu, M., Alsiwat, J.M., Ozcebe, G. Hysteretic Behavior of Anchorage Slip in R/C Members. *ASCE Journal of Structural Engineering*. 1992; **118** (9) 2439-2458.
- Setzler, E.J. Modeling the Behavior of Lightly Reinforced Concrete Columns Subjected to Lateral Loads. *M.S. Thesis*. The Ohio State University, Columbus, Ohio, 2005.
- Setzler, E.J., Sezen, H. Model for the Lateral Behavior of Reinforced Concrete Columns Including Shear Deformations. *Earthquake Spectra*. 2008; **24**(2) 493-511
- Sezen, H. Seismic Behavior and Modeling of Reinforced Concrete Building Columns. *Ph.D. Dissertation*. University of California, Berkeley, 2002.
- Sezen, H., Whittaker, A.S., Elwood, K.J., Mosalam, K.M. Performance of Reinforced Concrete and Wall Buildings during the August 17, 1999 Kocaeli, Turkey Earthquake, and Seismic Design and Construction Practice in Turkey. *Engineering Structures*. 2003; **25** (1): 103-114.

Sezen, H., Moehle, J.P. Bond-Slip Behavior of Reinforced Concrete Members. *fib-Symposium: Concrete Structures in Seismic Regions*. CEB-FIP, Athens, Greece, 2003.

Sezen, H., Moehle J.P. Seismic Tests of Concrete Columns with Light Transverse Reinforcement. *ACI Structural Journal* 2006; **103** (6) 842-849.

Sezen H., and Setzler E.J. Reinforcement Slip in Reinforced Concrete Columns. *ACI Structural Journal*. 2008; **105**(3) 280-289

Takeda, T., Sozen, M.A., Neilsen, N.N. Reinforced Concrete Response to Simulated Earthquakes. *Journal of the Structural Division, ASCE*. 1970; **96** (12), 2557-2573.

Vecchio, F.J., Collins, M.P. The Modified Compression-Field Theory for Reinforced Concrete Elements Subjected to Shear. *ACI Journal* 1986; **83** (2) 219-231.

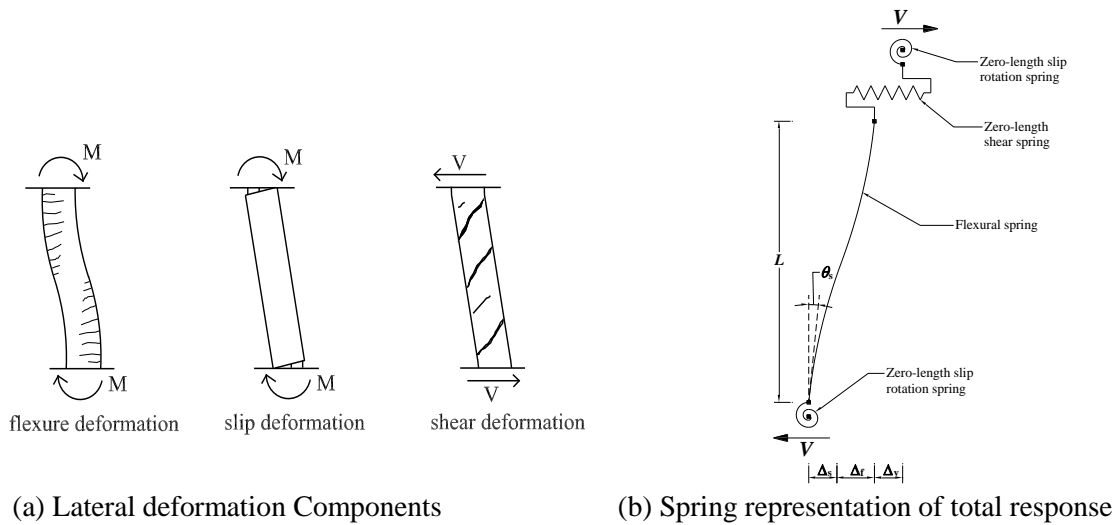


**Figure 1.** Lateral deformation of a reinforced concrete column

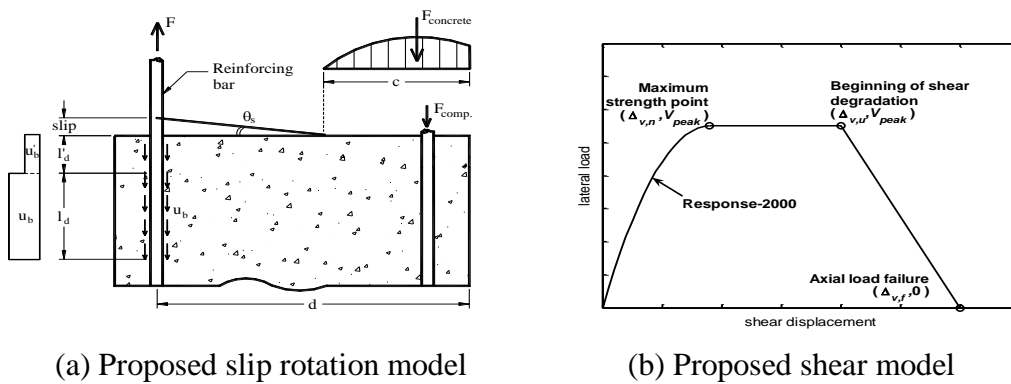
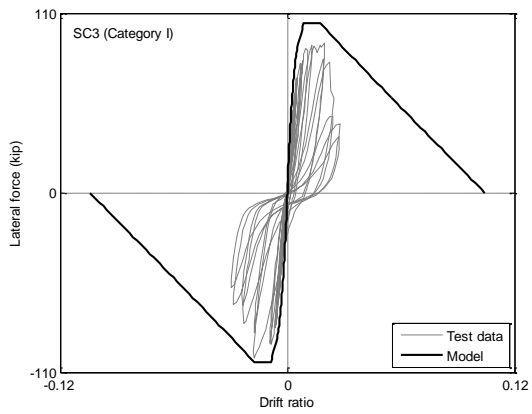
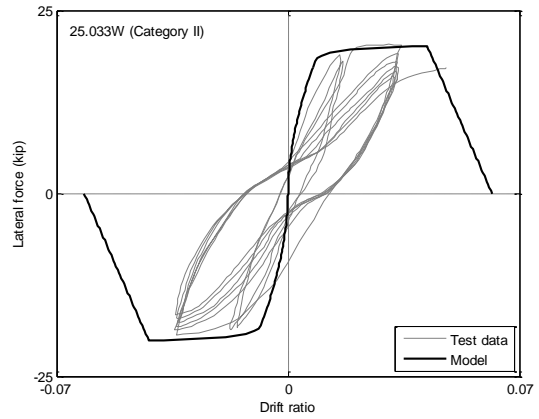


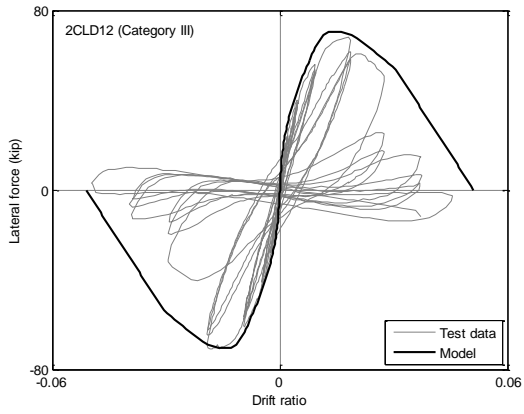
**Figure 2.** Proposed models for component deformations



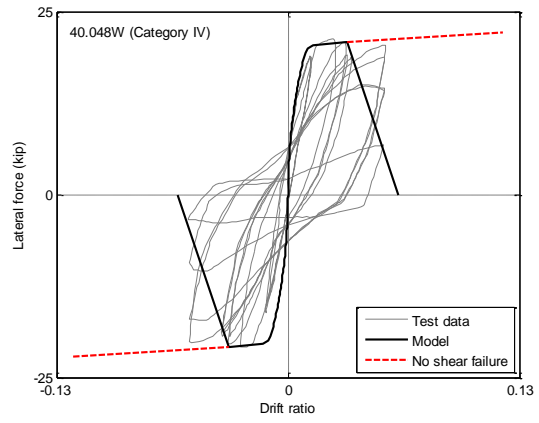
(a)



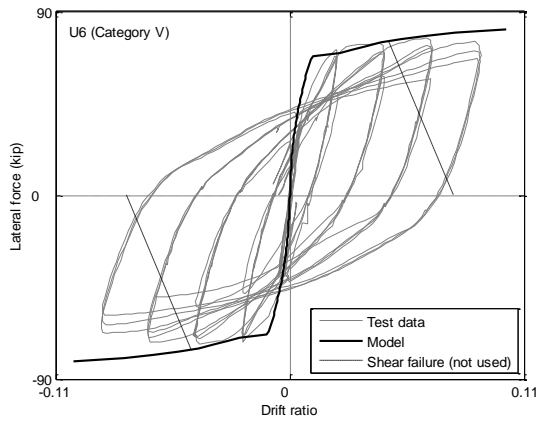
(b)



(c)

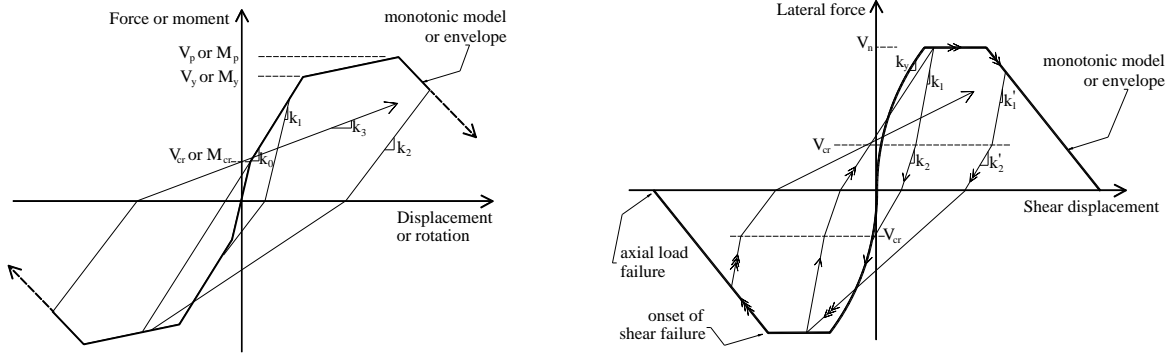


(d)



(e)

**Figure 3.** Model predictions and test data for the lateral displacement  
 (a) SC3, (b) 25.033W, (c) 2CLD12, (d) 40.048W, (e) U6



(a) Lateral force-flexural displacement

(b) Lateral force-shear displacement

**Figure 4:** Hysteretic rules for lateral force-displacement relationship

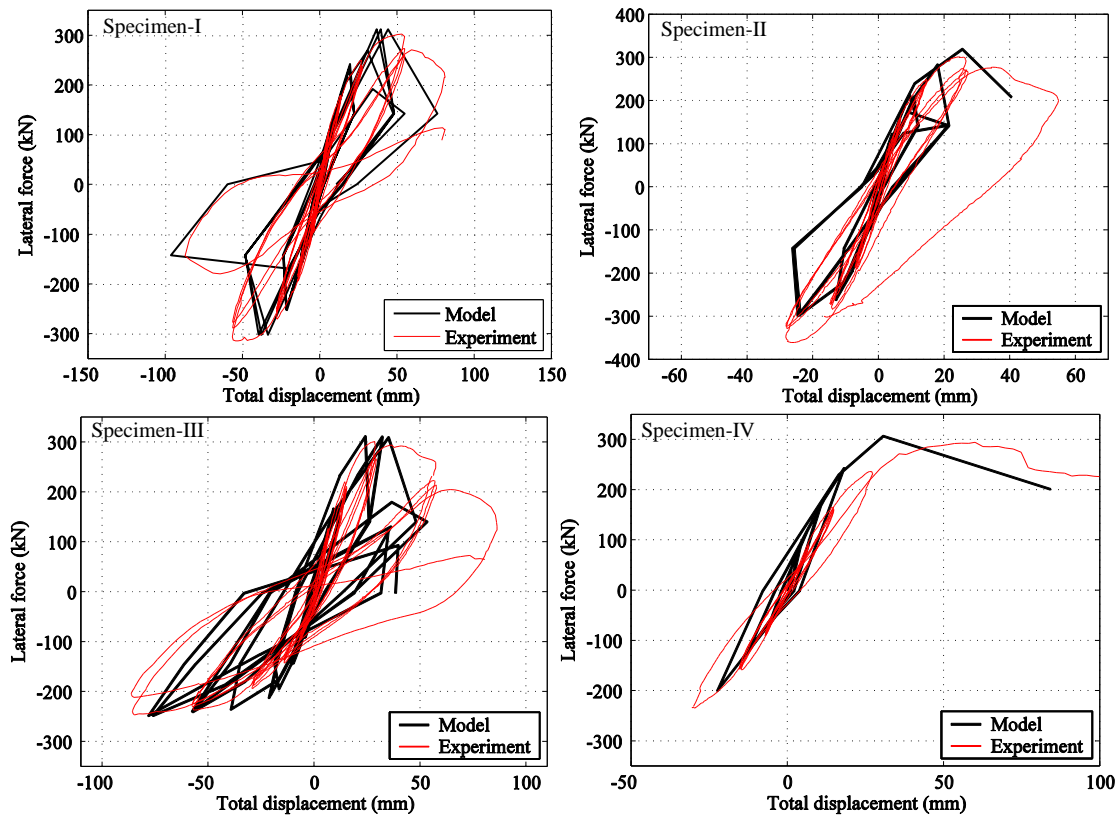


**Figure 5:** Total predicted and measured response of Columns tested by Sezen (2002)